IEEE Access
Multidisciplinary : Rapid Review : Open Access Journal

Received December 4, 2020, accepted January 8, 2021, date of publication January 21, 2021, date of current version February 2, 2021.

Digital Object Identifier 10.1109/ACCESS.2021.3053517

A Reduced Complexity Tensor Approach for Order Selection and Frequency Estimation

RUNYI YU, (Senior Member, IEEE), AND ERHAN A. INCE, (Member, IEEE)
Department of Electrical and Electronic Engineering, Eastern Mediterranean University, 99628 Gazimağusa, Turkey
Corresponding author: Runyi Yu (yu@ieee.org)

ABSTRACT This paper presents a reduced complexity tensor approach for order selection and subspace-based frequency estimation. The proposed covariance tensor based order selection algorithm, termed as CT-OS, uses singular values of the covariance tensor formed from the 1D noisy observations of multiple complex sinusoids. Experimental results show that the CT-OS algorithm is capable of providing accurate order selection under short observations and is robust under medium to high signal-to-noise ratios. The proposed covariance tensor based frequency estimator, termed as CT-FE, utilizes a singular vector matrix in the higher-order singular value decomposition of the covariance tensor. Experimental results show that the CT-FE outperforms the subspace alignment and separation algorithm (SAS-Est) and a recent two-stage order and frequency estimation algorithm. Furthermore, both theoretical analysis and experimental results demonstrate reduced computational complexity and time for the proposed CT-OS against the recent covariance tensor based order estimation algorithm CTB-OE. The CT-FE algorithm is also shown to enjoy reduced computational complexity and time when compared with the frequency estimator SAS-Est.

INDEX TERMS Covariance tensor, frequency estimation, generalized Kullback-Leibler divergence, high order singular value decomposition, order selection, subspace alignment and separation algorithm.

NOMENCLATURE

2S-Est	2-stage estimation
CT-OS	Covariance tensor based order selection
CT-FE	Covariance tensor based frequency estimation
CTB-OE	Covariance tensor based order estimation
HOSVD	High order singular value decomposition
MUSIC	MUltiple SIgnal Classification
PCOE	Percentage of correct order estimation
SAS-Est	Subspace alignment and separation based estimation
$\mathbb{C}$	Set of complex numbers
$\mathbb{R}$	Set of real numbers
Δf	Minimum frequency separation
$\boldsymbol{\mathcal{R}}$	Covariance tensor ($M \times M \times K$)
$\boldsymbol{\mathcal{S}}$	Core tensor
$\widehat{\mathbf{R}}$	Covariance matrix estimate ($M \times M$)
$D(\mathbf{p} \parallel \mathbf{q})$	Generalized Kullback-Leibler divergence of vector $\mathbf{p}$ to $\mathbf{q}$
N	Length of observation

The associate editor coordinating the review of this manuscript and approving it for publication was Wei-Wen Hu.

I. INTRODUCTION

Order selection and frequency estimation are fundamental problems that arise from many important applications in fields such as telecommunications, signal processing, and power systems [1]. Most model-based methods require the selection of a single or several integer-valued parameters, often referred to as model order. The number of sinusoidal components in a noisy signal or the number of source signals striking on a sensor array are two examples of such integer-valued parameters. According to [2], the most commonly used order selection method is the maximum likelihood method (MLM). Akaike information criteria, generalized information criteria, and Bayesian information criteria are some rules that can be used together with MLM. Frequency estimation, also known as line spectral estimation, can generally be grouped into two classes; namely, parametric and non-parametric methods [3], [4]. Non-parametric methods require no assumptions about data sequence model and respective algorithms such as those based on periodogram or FFT have small computational cost. However, they are not capable of resolving closely spaced frequencies and tend to introduce bias in the frequency estimates. Parametric methods on the other hand are known to provide better resolution and can resolve closely spaced spectral peaks. Typical examples of parametric algorithms include the well-known MUltiple SIgnal Classification (MUSIC) [5], its variations (such as the root-MUSIC [6], ESPRIT [7], E-MUSIC [8], and SAS-Est [9]), and the discrete polynomial phase transform based parameter estimation algorithms [10], [11]. Combining the ideas behind these two classes, an efficient 2-stage order and frequency estimation algorithm (abbreviated as 2S-Est herein) was recently presented in [12]. This algorithm has also been extended for 2D signals in [13]. Note, however, that all these algorithms perform well only when the observation data are sufficiently long and their performances would deteriorate under short observations.

Aiming primarily at processing short observation data and motivated by the tensor approach of [14] for exponential data fitting, we recently proposed in [15] a covariance tensor based order estimation algorithm (termed as CTB-OE therein). It was shown via simulations that the CTB-OE is capable of providing better performance than classical approaches since it allows exploitation of the redundancy introduced in the covariance tensor. The approach was established based on our observation that contributions of sinusoids and noise are separable in the incremental Frobenius norms of the leading principal subtensors of the core tensor in high order singular value decomposition (HOSVD).

In the literature, the tensor approach has also been used in multi-dimensional frequency estimation and order selection methods such as multi-dimensional folding [16], rank reduction estimation [17], decoupled root-MUSIC [18], higher-order singular value decomposition [19], and the latest unitary root-MUSIC based on tensor mode-R algorithm [20]. It is pointed out that in these studies the data are already in tensor form and of large size. Furthermore, algorithms that are specifically designed for multi-dimensional models are known to require large number of snapshots [21].

In efforts to gain theoretical understanding and to reduce the computational complexity of the CTB-OE [15], we have developed a new covariance tensor based order selection algorithm which we refer to as CT-OS. We have also derived a covariance tensor based algorithm for frequency estimation, which we refer to as CT-FE. Both algorithms are illustrated in the respective flowcharts in Figure 1 and shall be detailed in the next section. We show that the two algorithms are efficient and effective for short observations, and that they have reduced computational complexity. The contributions of this work are as follows:

1) We present a new order selection algorithm, i.e., CT-OS. Its improvement over the CTB-OE [15] is twofold: i) in theory, the CT-OS is justified based on a relationship between the singular values of covariance matrix and the 1-mode singular values of the covariance tensor; and ii) in computation, the CT-OS is shown to enjoy a reduced computational complexity since it avoids computing the core tensor in the HOSVD. A three-quarter reduction in computational complexity over the CTB-OE has been demonstrated both analytically and via simulations.

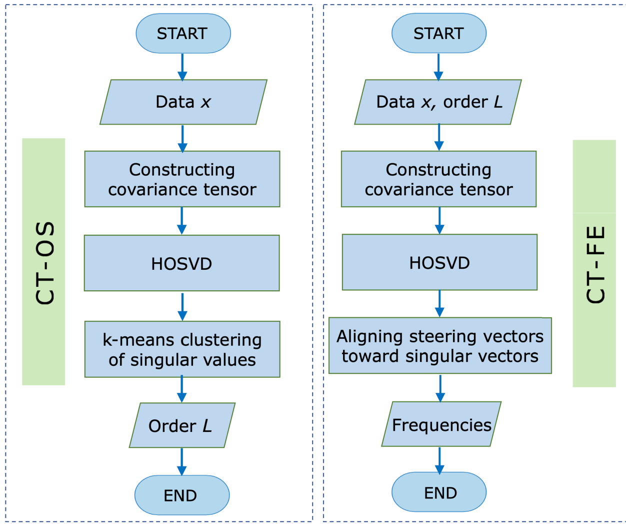

FIGURE 1. Flowcharts of the proposed covariance tensor based order selection and frequency estimation (CT-OS and CT-FE).

2) We also present a novel covariance tensor based frequency estimation algorithm, i.e., CT-FE. Benefiting from the redundancy that the covariance tensor offers, the CT-FE allows good frequency estimates that are close to the Cramer-Rao lower bound (CRLB) [22]. The CT-FE also has a reduced computational complexity when compared with the SAS-Est, thanks to the good performance of the CT-OS and a modification in the frequency searching space of the optimization problem.

Experiments under additive white Gaussian noise (AWGN) show that the proposed CT-OS allows accurate model order selection under medium to large SNRs. It also has been demonstrated that CT-OS allows significant improvements over other model order selection algorithms such as MUSIC, ESPIRIT+MAP, and E-MUSIC. The improvements are particularly notable at high order scenarios or under short observation sizes. Experiments on frequency estimates also demonstrate the advantages of the CT-FE over two recent frequency estimation algorithms, namely, SAS-Est [9] and 2S-Est [12]. In addition, the CT-OS and CT-FE are also applied on a real signal, namely, a piece of guitar audio recording.

The remainder of this paper is organized as follows: The problem statement and formation of covariance tensor are provided in Section II. Section III details the proposed CT-OS and CT-FE algorithms and discusses their computational complexities. Experimental results are provided in Section IV. Finally, conclusions are drawn in Section V.

Throughout the paper, scalars are denoted by italic Roman letters (e.g., a) or Greek letters (e.g., σ), boldface lowercase letters are used for vectors (e.g., $\mathbf{x}$), boldface capital letters denote matrices (e.g., $\mathbf{M}$), and tensors are denoted by capital bold calligraphic letters (e.g., $\boldsymbol{\mathcal{R}}$). The starting index of arrays is set to be 0.

II. PROBLEM STATEMENT AND COVARIANCE TENSOR FORMATION

Consider a complex discrete-time signal modeled as a linear combination of several complex sinusoids contaminated by additive noise:

$$x_n = \sum_{\ell=0}^{L-1} a_\ell e^{j(2\pi f_\ell + \phi_\ell)} + w_n, \quad n = 0, 1, \ldots, N-1 \quad (1)$$

where L is the model order, N is the observation size, $f_\ell \in (0, 1)$ and $a_\ell > 0$ are the ℓth sinusoid's frequency (in Hz) and the amplitude respectively. It is assumed that phases ϕ_ℓ's are independent and uniformly distributed in $(-\pi, \pi]$, and that noise samples w_n are independent and stationary.

Our order selection and frequency estimation problems can be stated as follows: Given N samples of the noisy signal x in (1), estimate 1) the order L, and 2) the frequencies f_ℓ, $\ell = 0, 1, \ldots, L-1$.

In the sequel, we present a covariance tensor approach to the said problems. Given the 1D data x, we first form a 3D covariance tensor as illustrated in Figure 2. We start by cropping the data into K overlapping segments of length W:

$$\mathbf{x}_k = \left[x_k x_{k+1} \cdots x_{k+W-1}\right]^T \in \mathbb{C}^W, \quad k = 0, 1, \ldots, K-1 \quad (2)$$

where $W = N - K + 1$. Then, for the kth segment, an estimate of its covariance matrix can be obtained, for example, as

$$\widehat{\mathbf{R}}_k = \frac{1}{M+1} \sum_{\mu=0}^{M} \mathbf{x}_{k,\mu} \mathbf{x}_{k,\mu}^H \in \mathbb{R}^{M \times M} \quad (3)$$

where $M = \lfloor W/2 \rfloor$, the superscript H denotes the Hermitian operator, and

$$\mathbf{x}_{k,\mu} = \left[x_{k+\mu}\ x_{k+\mu+1} \cdots x_{k+\mu+M-1}\right]^T \in \mathbb{C}^M \quad (4)$$

for $\mu = 0, 1, \ldots, M$. Finally, by up all the covariance matrices, we form a 3-way K-layer covariance tensor $\mathcal{R} \in \mathbb{R}^{M \times M \times K}$.

III. A TENSOR APPROACH TO ORDER SELECTION AND FREQUENCY ESTIMATION

This section describes the proposed covariance tensor based order selection (CT-OS) and frequency estimation (CT-FE) algorithms. It also discusses their computational complexities. We begin by introducing the HOSVD of covariance tensor $\mathcal{R}$.

A. HOSVD OF COVARIANCE TENSOR

Under the HOSVD [23], the 3D covariance tensor $\mathcal{R}$ can be expressed as

$$\mathcal{R} = \mathcal{S} \times_1 \mathbf{U}_1 \times_2 \mathbf{U}_2 \times_3 \mathbf{U}_3 \quad (5)$$

where $\mathcal{S} \in \mathbb{C}^{M \times M \times K}$ is the core tensor which satisfies the all-orthogonality and the ordering properties, $\mathbf{U}_d$, $d = 1, 2, 3$, are orthonormal matrices of d-mode singular vectors of $\mathcal{R}$, and operator $\times_d$ represents the mode-d product of tensor with matrix, $d = 1, 2, 3$. Let $\mathcal{S}_{i_d=\mu}$ denote the subtensors of $\mathcal{S}$ in which the dth index is fixed to be μ, where

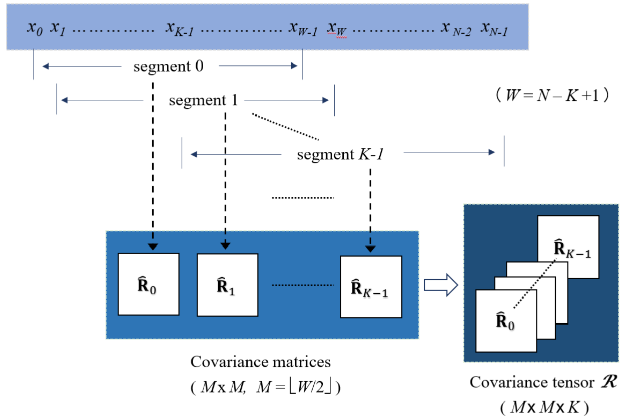

FIGURE 2. Formation of covariance tensor $\mathcal{R}$ from 1D discrete-time signal $\boldsymbol{x}$.

$\mu = 0, 1, \ldots, I_d - 1$, with $I_1 = I_2 = M$ and $I_3 = K$. Then the ordering property implies their Frobenius norms can be ordered as

$$\|\mathcal{S}_{i_d=0}\|_F \geq \|\mathcal{S}_{i_d=1}\|_F \geq \cdots \geq \|\mathcal{S}_{i_d=I_d-1}\|_F, \ d = 1, 2, 3. \quad (6)$$

As an example, if $d = 1$, (6) becomes

$$\|\mathcal{S}(0, :, :)\|_F \geq \|\mathcal{S}(1, :, :)\|_F \geq \cdots \geq \|\mathcal{S}(M-1, :, :)\|_F. \quad (7)$$

Furthermore, these Frobenius norms are equal to the d-mode singular values $\sigma_\mu^{(d)}$ of $\mathcal{R}$, i.e.,

$$\|\mathcal{S}_{i_d=\mu}\|_F = \sigma_\mu^{(d)}, \quad d = 1, 2, 3; \ \mu = 0, 1, \ldots, I_d - 1 \quad (8)$$

which are defined as the singular values of the d-mode unfolding matrix $\mathcal{R}_{(d)}$ of tensor $\mathcal{R}$.

We shall show in the sequel that this ordering property allows a simplified order selection based on only the 1-mode singular values $\sigma_\mu^{(1)}$'s. Moreover, an efficient frequency estimator can also be developed by using singular vector matrix $\mathbf{U}_1$.

B. COVARIANCE TENSOR BASED ORDER SELECTION (CT-OS)

For the purpose of theoretical analysis and under the stationarity assumption on x, it is reasonable to suppose that estimate in (3) yields approximately the same covariance matrix $\widehat{\mathbf{R}} \in \mathbb{R}^{M \times M}$ for $k = 0, \ldots, K-1$. As a result, the 1-mode unfolding matrix of the covariance tensor $\mathcal{R}$ has the following block structure:

$$\mathcal{R}_{(1)} \approx \underbrace{\left[\widehat{\mathbf{R}}\ \widehat{\mathbf{R}} \cdots \widehat{\mathbf{R}}\right]}_{K \text{ blocks}}. \quad (9)$$

Let a singular value decomposition of $\widehat{\mathbf{R}}$ be given as

$$\widehat{\mathbf{R}} = \mathbf{U}\Sigma\mathbf{U}^T \quad (10)$$

where $\mathbf{U} \in \mathbb{R}^{M \times M}$ is a singular vector matrix that is orthonormal and $\Sigma \in \mathbb{R}^{M \times M}$ is diagonal with elements being singular values of $\widehat{\mathbf{R}}$. Denote these values as $\sigma_0 \geq \sigma_1 \geq \cdots \geq$

Algorithm 1 Covariance Tensor Based Order Selection (CT-OS)

Input: N samples of signal x
Output: Model order L

Set the number of layers K
Estimate covariance matrices $\widehat{\mathbf{R}}_k$, $k = 0, 1, \ldots, K-1$, and form the covariance tensor $\boldsymbol{\mathcal{R}}$
Calculate the 1-mode singular values $\sigma_\mu^{(1)}$, $\mu = 0, 1, \ldots, M-1$
Apply the k-means clustering to $\{\sigma_\mu^{(1)}\}_{\mu=0}^{M-1}$ to obtain two clusters
Take L to be the size of the cluster with larger singular values
while $|\sigma_L^{(1)} - (m_s + m_n)/2| \leq |\sigma_L^{(1)} - m_n|$ **do**
    $L \leftarrow L + 1$
end while

$\sigma_{M-1} \geq 0$. In view of (9), it can be shown that the 1-mode singular values of $\boldsymbol{\mathcal{R}}$ are related to those of matrix $\widehat{\mathbf{R}}$ as[1]

$$\sigma_\mu^{(1)} \approx \sqrt{K}\sigma_\mu, \quad \mu = 0, 1, \ldots, M-1. \tag{11}$$

To motivate our CT-OS algorithm, we recall that if $\widehat{\mathbf{R}}$ estimates the covariance matrix of signal x accurately, then its singular values are separated in terms of the amplitudes a_ℓ's of the sinusoids and the power σ^2 of the noise as [1]

$$\sigma_\mu = \begin{cases} a_\mu + \sigma^2, & \mu = 0, 1, \ldots, L-1 \\ \sigma^2, & \mu = L, \ldots, M-1. \end{cases} \tag{12}$$

This implies that order L can be estimated via this separation property of σ_μ's.

In view of relationship (11), we can set L to be the number of large 1-mode singular values $\sigma_\mu^{(1)}$'s. These large elements can be selected using the k-means clustering algorithm [24] which separates $\{\sigma_\mu^{(1)}\}_{\mu=0}^{M-1}$ into two clusters: a signal cluster of large elements and a noise cluster with the remaining smaller elements. Order L is then taken to be the number of elements in the signal cluster. Through experiments, we observe that the simple k-means clustering sometimes under-estimates the model order. We thus fine-tune the order by comparing the largest element $\sigma_L^{(1)}$ of the noise cluster against the means $m_s = \text{mean}\{\sigma_\mu^{(1)}\}_{\mu=0}^{L-1}$ and $m_n = \text{mean}\{\sigma_\mu^{(1)}\}_{\mu=L}^{M-1}$ of the two clusters. If this element is closer to the average of the two means than to m_n, then it is moved into the signal cluster. This comparison can be repeated for the two updated clusters until no further tuning is necessary. The pseudocode for the proposed CT-OS is provided in Algorithm 1.

C. COVARIANCE TENSOR BASED FREQUENCY ESTIMATION (CT-FE)

We now assume that L is accurately estimated by the CT-OS. Under the structural property (9), the left singular vectors of $\boldsymbol{\mathcal{R}}_{(1)}$ are found to be approximately identical to those of covariance matrix $\widehat{\mathbf{R}}$. Furthermore, if the covariance estimation is accurate, singular vector matrix $\mathbf{U}_1$ of HOSVD in (5) is identical to $\mathbf{U}$ in (10). This implies that $\mathbf{U}_1$ can be used to estimate the frequencies of x based on their relation to the steering matrix [1]

$$\mathbf{A} = \left[\mathbf{a}_0 \cdots \mathbf{a}_{L-1}\right] \in \mathbb{C}^{M \times L} \tag{13}$$

where steering vector $\mathbf{a}_\ell$ is defined in terms of the corresponding frequency f_ℓ as follows:

$$\mathbf{a}_\ell = \left[1 \; e^{j2\pi f_\ell} \; \cdots \; e^{j(M-1)2\pi f_\ell}\right]^T \in \mathbb{C}^M \tag{14}$$

for $\ell = 0, 1, \ldots, L-1$.

Let $\mathbf{S}$ be the submatrix composed of the first L columns of $\mathbf{U}_1$, i.e.,

$$\mathbf{S} = \mathbf{U}_1(:, 0 : L-1). \tag{15}$$

When the covariance matrix $\mathbf{R}$ is precisely estimated, the signal subspace $\mathcal{C}(\mathbf{S})$,[2] and the steering subspace $\mathcal{C}(\mathbf{A})$ are identical. This suggests that we can estimate the frequencies by aligning $\mathcal{C}(\mathbf{S})$ toward $\mathcal{C}(\mathbf{A})$ [9]. The closeness of these two subspaces can be characterized in terms of their principal angles θ_ℓ, $\ell = 0, 1, \ldots, L-1$. These principal angles can be determined via the leading singular value s_ℓ's of $\mathbf{S}\mathbf{S}^+\mathbf{A}\mathbf{A}^+$ as $\theta_\ell = \cos^{-1}(s_\ell)$, since $\mathbf{S}\mathbf{S}^+$ and $\mathbf{A}\mathbf{A}^+$ are the orthogonal projection matrix on $\mathcal{C}(\mathbf{S})$ and $\mathcal{C}(\mathbf{A})$, respectively.[3] Note that when $\mathcal{C}(\mathbf{S}) = \mathcal{C}(\mathbf{A})$, all L angles between $\mathcal{C}(\mathbf{S})$ and $\mathcal{C}(\mathbf{A})$ are equal to zero. For the purpose of frequency estimation, we shall make the L angles as small (close to zero) as possible.

If the covariance matrix estimate is precise, then $\mathcal{C}(\mathbf{S}) = \mathcal{C}(\mathbf{A})$, thus $\theta_\ell = 0$ and $\mathbf{s}_\ell = 1$, $\ell = 0, 1, \ldots, L-1$. If this is not the case, then $\mathcal{C}(\mathbf{S}) \neq \mathcal{C}(\mathbf{A})$ and $0 \leq \mathbf{s}_\ell \leq 1$, $\ell = 0, 1, \ldots, L-1$. Aligning signal subspace $\mathcal{C}(\mathbf{S})$ toward steering subspace $\mathcal{C}(\mathbf{A})$ can be realized by pulling vector

$$\mathbf{s} = \left[s_0^2 \cdots s_{L-1}^2\right]^T \tag{16}$$

toward vector

$$\mathbf{1} = \left[1 \cdots 1\right]^T \in \mathbb{R}^L. \tag{17}$$

The degree of this non-alignment can be measured in terms of the generalized Kullback-Leibler divergence [25] between the two vectors. Recall that the generalized Kullback-Leibler divergence of two L-dimensional non-negative vectors $\mathbf{p} = \{p_\ell\}$ and $\mathbf{q} = \{q_\ell\}$ is defined as [25]

$$D(\mathbf{p}\|\mathbf{q}) = \sum_{\ell=0}^{L-1}\left(p_\ell \ln \frac{p_\ell}{q_\ell} - p_\ell + q_\ell\right). \tag{18}$$

Hence, the non-alignment measure between $\mathcal{C}(\mathbf{S})$ and $\mathcal{C}(\mathbf{A})$ can be written as

$$D(\mathbf{s}\|\mathbf{1}) = L - \sum_{\ell=0}^{L-1}(1 - \ln s_\ell^2)s_\ell^2. \tag{19}$$

It is easy to see that $0 \leq D(\mathbf{s}||\mathbf{1}) \leq L$ in general and that $D(\mathbf{s}||\mathbf{1})$ attains the minimum of 0 if and only if $\mathcal{C}(\mathbf{S}) = \mathcal{C}(\mathbf{A})$

[1] Since $\widehat{\mathbf{R}}$ is Hermitian, the 2-mode singular values of $\boldsymbol{\mathcal{R}}$ are the same as the 1-mode singular values; i.e., $\sigma_\mu^{(2)} = \sigma_\mu^{(1)}$, $\mu = 0, 1, \ldots, M-1$.

[2] $\mathcal{C}(\cdot)$ denotes the column space of "$\cdot$".

[3] The superscript "$+$" denotes the Moore–Penrose pseudoinverse.

Algorithm 2 Covariance Tensor Based Frequency Estimation (CT-FE)

Input: N samples of signal x and model order L
Output: Frequency estimates $\widehat{f}_0, \widehat{f}_1, \ldots, \widehat{f}_{L-1}$

1: Set the number of layers K
2: Estimate covariance matrices $\widehat{\mathbf{R}}_k$, $k = 0, 1, \ldots, K-1$, and form the covariance tensor $\boldsymbol{\mathcal{R}}$
3: Compute orthogonal matrix $\mathbf{U}_1$ and let $\mathbf{S} = \mathbf{U}_1(:, 0 : L-1)$
4: Define non-alignment measure $D(\mathbf{s} \parallel \mathbf{1})$ as in (19), where $\mathbf{s}$ is given in terms of the L leading singular values of $\mathbf{S}\mathbf{S}^{+}\mathbf{A}\mathbf{A}^{+}$ as in (16) with $\mathbf{A}$ being the steering matrix dependent on frequency $f_0, f_1, \ldots, f_{L-1}$
5: Minimize $D(\mathbf{s} \parallel \mathbf{1})$ subject to the constraint (21) to obtain estimates $\widehat{f}_0, \widehat{f}_1, \ldots, \widehat{f}_{L-1}$

(when $\mathbf{s} = \mathbf{1}$). Note that through steering matrix $\mathbf{A}$ of (13), measure $D(\mathbf{s}\|\mathbf{1})$ is function of f_ℓ, $\ell = 0, 1, \ldots, L-1$. As a result, the least divergence between $\mathcal{C}(\mathbf{S})$ and $\mathcal{C}(\mathbf{A})$ is attained at the frequencies of signal x in (1). This implies that these frequencies can be estimated as solution to the following minimization problem:

$$\widehat{\mathbf{f}} = \arg\min_{\mathbf{f} \in \mathbb{F}} D(\mathbf{s}\|\mathbf{1}) \tag{20}$$

where,

$$\mathbb{F} = \{\mathbf{f} = [f_0 f_1 \cdots f_{L-1}]^T : \; 0 < f_0 < f_1 < \cdots < f_{L-1} < 1\} \tag{21}$$

is the set of searching vectors of frequencies. The pseudocode for the CT-FE is provided in Algorithm 2.

D. COMPUTATIONAL COMPLEXITY

First, it is pointed out that compared with the CTB-OE [15], the proposed CT-OS enjoys a significantly reduced computational complexity. Consider CT-OS first. The complexity for singular value decomposition of $\boldsymbol{\mathcal{R}}_{(1)}$ is $O(M^3 K)$; and the complexity of the k-clustering is $O(M^2)$. Hence, the overall complexity of the CT-OS is equal to $O(M^3 K + M^2)$, or approximately $O(M^3 K)$ since $M^2 \ll M^3 K$. On the other hand, the CTB-OE requires the core tensor $\boldsymbol{\mathcal{S}}$, which involves computing the orthogonal matrices $\mathbf{U}_d$, $d = 1, 2, 3$, and additional three matrix multiplications. In view of the dimensions of the unfolding matrices of $\boldsymbol{\mathcal{R}}$, the complexity for computing $\boldsymbol{\mathcal{S}}$ is found to be $O(4M^3 K + 2M^2 K^2)$. In addition, computing Frobenius norms of the leading principal subtensors of $\boldsymbol{\mathcal{S}}$ has a complexity of $O(\frac{1}{3}M^3 K)$. As a result, the CTB-OE has an overall complexity of $O(4\frac{1}{3}M^3 K + 2M^2(K^2+1))$, which is approximately equal to $O(4\frac{1}{3}M^3 K)$ when $K \ll 2\frac{1}{6}M$ (thus $2M^2(K^2+1)) \ll 4\frac{1}{3}M^3 K)$.

The above complexity analysis results are summarized in Table 1. Roughly speaking, the computational load of CT-OS is seen to be slightly less than one quarter of that of the CTB-OE. In other words, it enjoys a reduction of more than three quarters. Consider one example where $N = 128$ and $K = 9$. We now have $M = 60$, and the overall complexity orders of CTB-OE and CT-OS are calculated to be $O(9,010,800)$ and $O(1,947,000)$ (or $O(8,424,000)$ and $O(1,944,000)$ approximately) respectively, giving a reduction of 76.9% (or 78.4% if the approximate formulas are used).

TABLE 1. Complexity Order of CTB-OE and CT-OS.

	HOSVD	Norm Computing	Clustering	Overall	Overall (if $K << 13M/6$)
CTB-OE	$4M^3K + 2M^2K^2$	$\frac{1}{3}M^3K$	M^2	$4\frac{1}{3}M^3K + M^2(2K^2+1)$	$4\frac{1}{3}M^3K$
CT-OS	M^3K	(n/a)	M^2	$M^3K + M^2$	M^3K

The size of the covariance tensor is $M \times M \times K$, where K denotes the number of covariance matrices and $M = \lfloor (N-K+1)/2 \rfloor$ with N being the length of observation data.

Similarly, the CT-FE is also shown to enjoy a significantly reduced computational load when compared with the SAS-Est algorithm [9], which aligns the steering subspace toward the signal subspace and simultaneously away from the noise subspace. Note that major computations for both CT-FE and SAS-Est are spent in solving the respective minimization problem. Thanks to the preceding CT-OS which renders a good selection for the model order, minimization in CT-FE is only over frequencies; whereas the SAS-Est needs to carry out a joint minimization over order and frequencies. As a result, the CT-FE would require less computation than the SAS-Est, as the objective functions in both algorithms are essentially the same in terms of the frequency argument. Moreover, recall that the searching space of SAS-Est is the entire hypercube $(0, 1)^L$, whereas the searching space of CT-FE reduces to only a small fraction ($1/2^{L-1}$ in volume) of the searching hypercube because of the linear inequalities in (21).

In Section IV we shall also demonstrate the significant saving of both CT-OS and CT-FE in computation-time over CTB-OE and SAS-Est, respectively.

IV. EXPERIMENTAL RESULTS

In this section the improvements introduced by the proposed reduced-complexity order selection and frequency estimation algorithms are demonstrated via simulations. We evaluate the performance of the proposed CT-OS and CT-FE algorithms for synthetic multiple complex sinusoids under AWGN. A guitar audio recording is also studied for their applicability to real-life signals.

The performances are measured in terms of the percentage of correct order estimation (PCOE) and mean square error (MSE) respectively. The CT-OS was compared against some subspace algorithms such as MUSIC [26], ESPRIT + MAP [7], E-MUSIC [8], SAS-Est [9], the recent CTB-OE [15] and 2S-Est [12]. The CT-FE was compared against SAS-Est [9] and 2S-Est [12], and in reference to the CRLB. In view of the recommendation in [15], the number of layers was chosen to be $K = 9$ in all experiments. All minimization problems are solved using the MATLAB function `fmincon`.

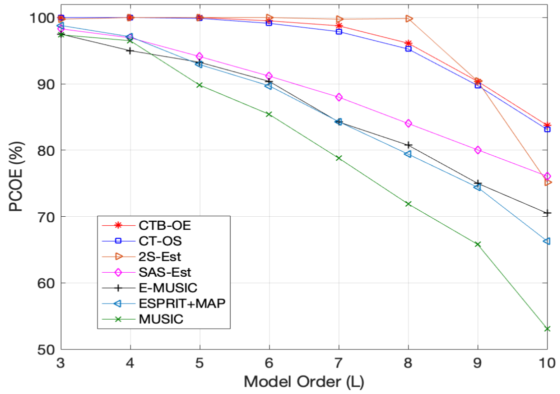

FIGURE 3. **PCOE comparison of the proposed CT-OS and some order selection algorithms under various model orders. [$\Delta f = 0.015$, SNR $= 20$dB, $N = 128$].**

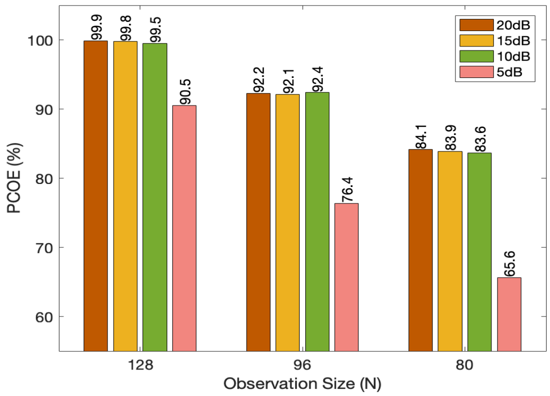

FIGURE 4. **PCOE performance of the proposed CT-OS under various observation sizes and SNR values. [$L = 5$, $\Delta f = 0.015$, $N = 128, 96, 80$].**

A. ORDER SELECTION

We first examined how the CT-OS algorithm would perform under various model orders. Figure 3 gives the PCOE results for model orders $L = 3, 4, \ldots, 10$, obtained from 400 Monte Carlo simulations. Note that, for all model orders considered, the performance of the CT-OS is over those of MUSIC, ESPRIT+MAP, E-MUSIC and SAS-Est, and is on a par with CTB-OE. In addition, the drop rate in PCOE at $L \geq 9$ is slower for CT-OS when compared with 2S-Est. For model orders 3 to 6 both 2S-Est and CT-OS have similar performances. At orders 7 to 8 the 2S-Est has an edge over CT-OS. At order $L = 9$ their performances become same (the curves cross each other) and at $L = 10$ the CT-OS has the highest PCOE, giving 7% edge over SAS-Est and 8% over 2S-Est.

Next, we studied the performance of the CT-OS algorithm under various observation sizes. For model order $L = 5$ and a minimum frequency separation of $\Delta f = 0.015$, which is the smallest admissible frequency difference between any frequency pair. Figure 4 depicts the PCOE values of the CT-OS under observation sizes of $N = 128, 96$, and 80 and SNR values of 20, 15, 10, and 5dB (each with 400 runs). The results depicted in Figure 4 indicate that, even with a 25% reduction (from $N = 128$ to $N = 96$) in observation size the CT-OS can still achieve 92% estimation accuracy under SNR values of 20, 15, and 10dB. When the observation size is further reduced to $N = 80$ (a 37.5% reduction from $N = 128$), the CT-OS algorithm would still deliver approximately 84% accuracy. Note that when $N = 96$, $L = 5$ and SNR$= 20$dB, the MUSIC and E-MUSIC algorithms would respectively get only 6.7% and 50% estimation accuracy [15].

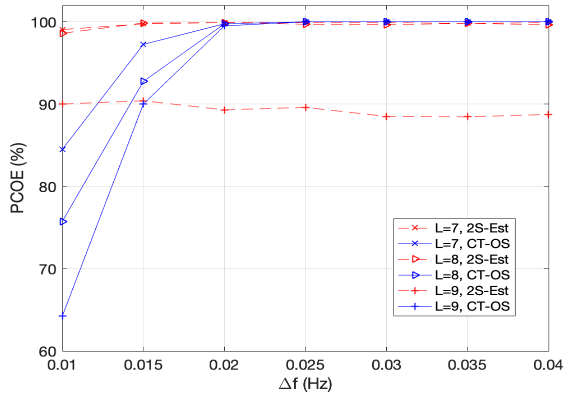

FIGURE 5. **PCOE comparison between CT-OS and 2S-Est algorithms under various model orders and Δf values. [$L = 7, 8, 9$, SNR$= 20$dB, $N = 128$].**

Figure 5 depicts the PCOE comparison between proposed CT-OS and the recent 2S-Est algorithms over a range of Δf values. In the experiment Δf is varied from 0.01 to 0.05 with steps of 0.005 and the PCOE is obtained for model orders of L = 7, 8 and 9. It is seen that the 2S-Est generally results in higher PCOE at $\Delta f \leq 0.015$ values, especially for model orders $L = 7$ and $L = 8$. However, for model order $L = 9$, the CT-OS consistently yields a PCOE of 100% for $\Delta f \geq 0.02$; whereas the 2S-Est gives some smaller value of 89%.

In the above experiments, the amplitudes of complex sinusoids were all assumed to be unity. We also tested the robustness of the CT-OS under none-unity amplitudes. We let the amplitudes be subject to variation up to an assumed percentage from the unity amplitude. The PCOE results depicted in Figure 6 shows that the CT-OS algorithm allows 30% variation for model orders from 3 to 7. Furthermore, performance with a 10% variation is almost as good as the one with unity amplitudes over all model orders tested.

B. FREQUENCY ESTIMATION

We now turn to the frequency estimation. Figure 7 depicts the MSE comparison between the proposed CT-FE algorithm and the SAS-Est [9] under various observation sizes and SNRs. All experiments assume that $L = 3$ and $\Delta f = 0.015$. The MSE for each frequency at a particular SNR was obtained from 200 Monte Carlo simulations. We observe that at $N = 128$ and 96, the MSE curves of the SAS-Est are parallel to the CRLB when SNR $\geq$ 5dB. If SNR $\leq$ 0dB, they all diverge away from the CRLB and the MSE is always above 10^{-4}. On the other hand, even at SNR$=$ 0dB the MSE curves of the CT-FE are still parallel to the CRLB. At $N = 80$,

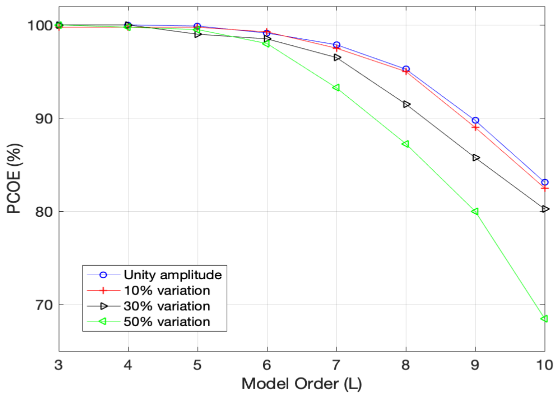

FIGURE 6. PCOE with unity and non-unity amplitudes. [$\Delta f = 0.015$, SNR $= 20$dB, $N = 128$].

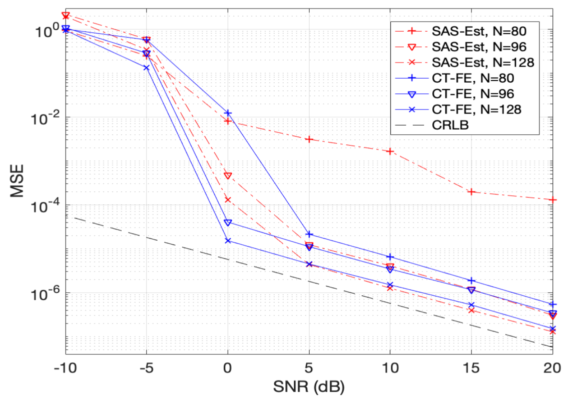

FIGURE 7. MSE comparison of the proposed CT-FE and SAS-Est under various SNR values and observation sizes. [$L = 3$, $\Delta f = 0.015$].

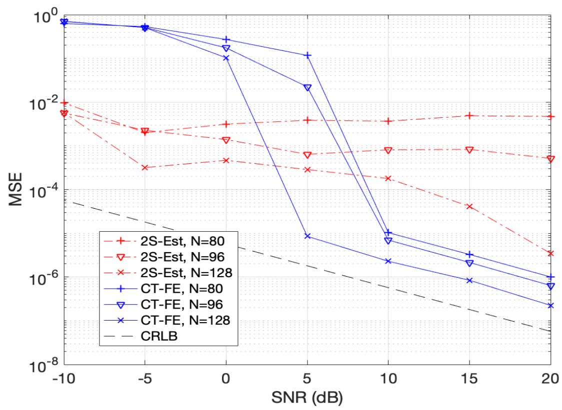

FIGURE 8. MSE comparison of the proposed CT-FE and 2S-Est under various SNR values and observation sizes. [$L = 5$, $\Delta f = 0.015$].

the CT-FE yields significant improvements under high SNR values (greater than or equal to 5dB) and the MSEs are only approximately 1% of those of the SAS-Est.

The proposed CT-FE algorithm was also compared against the 2S-Est [12] for the five-sinusoid case ($L = 5$). The results (also of 200 runs) are shown in Figure 8. It is seen that the MSE curves of the 2S-Est are all far above the CRLB, indicating that the 2S-Est is not suitable for short observations. The CT-FE on the other hand yields MSE close to the CRLB when SNR $\geq$ 10dB for $N = 96$, 80 and SNR $\geq$ 5dB for $N = 128$. This again shows that CT-FE is robust and performs well even under short observations.

C. FURTHER EXPERIMENTS: A GUITAR AUDIO SIGNAL

The proposed order and frequency estimation algorithms CT-OS and CT-FE were also tested using some real data obtained by playing notes C, E, A and D consecutively on a classical guitar and taking an audio recording (with a sampling frequency of 44100 Hz). For the purpose of our experiment, the recorded audio recording was first decimated using a down-sampling factor of 20 to have fewer samples. The decimated audio is then considered in our applications of the CT-OS and CT-FE. For any notes played on the fret board there would be a number of frequency components generated [27]. The frequencies include the fundamental frequency (also known as main pitch frequency), multiples of the fundamental frequency (often referred to as overtones or harmonics), and undertones which may occur due to vibration of the instrument or its parts [28]. Considering that the order and frequencies of the audio signal has a time-varying nature, we segmented the signal into overlapping sections and each section is then processed separately for the purpose of order selection and frequency estimation. One example of the decimated audio signal is shown in Figure 9(a), which also shows the centers of the segments of and overlaps (10%). Figure 9(b) shows the spectrogram of the audio wave. Each line on the spectrogram either indicates a fundamental frequency for the note played or its overtone/undertone. The number of lines in an observed section of the spectrogram can serve as a reference value of model order of the particular section of the audio signal. We then applied our CT-OS and CT-FE algorithms to every sections of the audio. In view of existence of multiple overtones in Guitar audio, the order selected using Algorithm 1 is further tuned so that the signal cluster is adequately separated from the noise cluster in the sense that the least element of the signal cluster is at least twice as large as the largest element of the noise cluster. The model orders and frequencies obtained are presented in Figures 9(c) and 9(d), respectively. It is seen that the frequency estimates in Figure 9(d) agree with the respective frequency lines in the spectrogram quite well. These results demonstrate the applicability of the proposed algorithms to a real-life signal.

D. COMPUTATIONAL TIME

A final experiment was carried out to compute the average run-times of the proposed CT-OS and CT-FE and to compare them with two related algorithms, namely, CTB-OE and SAS-Est. The PC used had a 2.4GHz Intel core i5 CPU supported by 8GB of RAM. Figure 10 shows average computation times obtained for the CT-OS and CT-FE and compares them with those of CTB-OE and SAS-Est. Since SAS-Est is a joint order and frequency estimator, we also considered

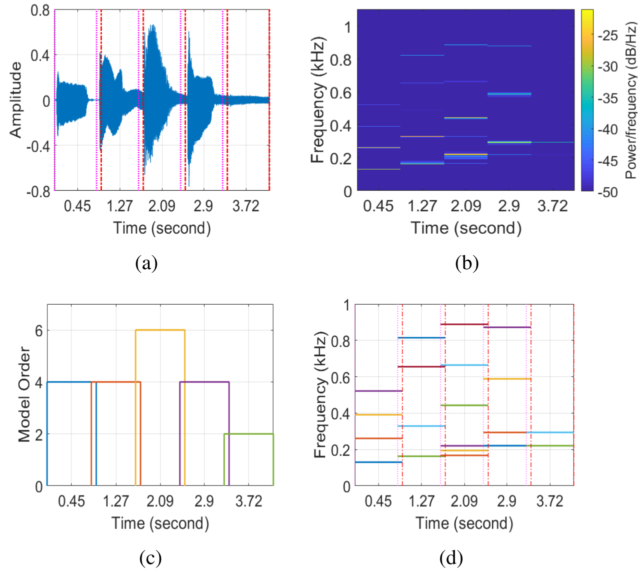

FIGURE 9. Experimental results on a guitar recording: (a) the audio wave, (b) its spectrogram, (c) the order selection, (d) the frequency estimation.

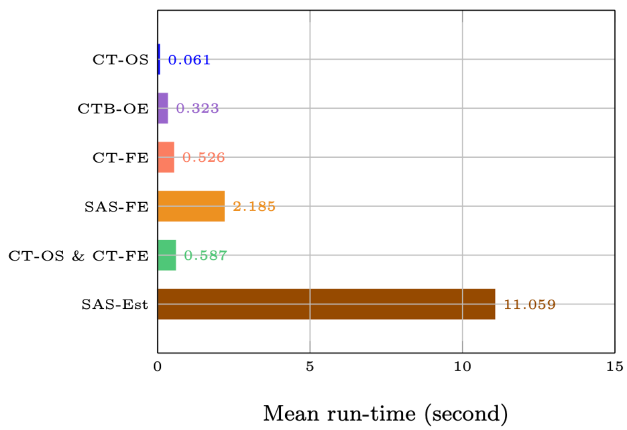

FIGURE 10. Comparison of average computation times [$L = 3$, $\Delta f = 0.015$, SNR $= 20$dB, $N = 128$].

its simplified version SAS-FE which takes a predetermined model order and estimates the frequencies only. All average times have been computed over 400 Monte Carlo simulations and under condition $L = 3$, $\Delta f = 0.015$, SNR $=$ 20dB, and $N = 128$ As shown in Figure 10, the CT-OS requires four times less computation time than CTB-OE. Furthermore, the average runtime for CT-FE is roughly one quarter of that of SAS-FE. A look at the average computation times for joint order and frequency estimation shows that the proposed CT-OS & CT-FE pair requires far less computational time than SAS-Est.

It should be pointed out that the execution times are dependent on machine configuration and programming skill. Nevertheless, considering the fact that the experiment was carried out on the same PC and implemented by the authors, and that the comparison results are in good agreement with complexity analysis results of Section III-D, it is reasonable to conclude the reduced computational time of the proposed new algorithms.

V. CONCLUSION

This paper proposed a reduced complexity covariance tensor based approach to order selection and frequency estimation for complex sinusoids in noise. Based on theoretical analysis, the proposed order selection algorithm CT-OS selects the order by clustering 1-mode singular values of a three-way covariance tensor. The proposed frequency estimator CT-FE aligns the signal subspace (which is obtained from 1-mode singular vectors of the covariance tensor) toward the steering vectors. Experimental results show that under short observations the CT-OS allows selection of the true model order and outperforms MUSIC, ESPRIT+MAP, and E-MUSIC. It is also demonstrated that the CT-FE algorithm is capable of yielding small mean-square error even at low SNRs, thus outperforming SAS-Est. Moreover, the CT-OS and CT-FE are also shown to enjoy reduced computational complexity and time when compared with the recent tensor based order estimator CTB-OE and subspace based frequency estimator SAS-Est.

It should be mentioned that the computational complexities of the two proposed estimation algorithms CT-OS and CT-FE are still high when compared with classical subspace based algorithms such as the MUSIC and its variants. Nevertheless, this may be regarded as a trade-off between achieving good performance in difficult scenarios (e.g., under short observation sizes) and computational cost. Future work on the two algorithms may focus on their theoretical performance analysis.

REFERENCES

[1] P. Stoica and R. Moses, *Introduction to Spectral Analysis*. Englewood Cliffs, NJ, USA: Prentice-Hall, 1997.
[2] P. Stoica and Y. Selen, "Model order selection: A review of information criterion rules," *IEEE Signal Process. Mag.*, vol. 21, no. 4, pp. 36–47, Jul. 2004.
[3] I. Santamaria, C. Panteleon, and J. Ibanez, "A comparative study of high-accuracy frequency estimation methods," *Mech. Syst. Signal Process.*, vol. 14, no. 5, pp. 1–16, 2000.
[4] H. Qiao, "Estimating the number of sinusoids in additive sub-Gaussian noise with finite measurements," *IEEE Signal Process. Lett.*, vol. 27, pp. 1225–1229, 2020.
[5] R. Schmidt, "Multiple emitter location and signal parameter estimation," *IEEE Trans. Antennas Propag.*, vol. 34, no. 3, pp. 276–280, Mar. 1986.
[6] B. D. Rao and K. V. S. Hari, "Performance analysis of root-music," *IEEE Trans. Acoust., Speech, Signal Process.*, vol. 37, no. 12, pp. 1939–1949, Dec. 1989.
[7] R. Roy and T. Kailath, "ESPRIT-Estimation of signal parameters via rotational invariance techniques," *IEEE Trans. on Acoust. Speech and Signal Process.*, vol. 37, no. 7, pp. 984–995, Jul. 1989.
[8] E. A. Ince, R. Yu, and A. Hocanin, "Entropy-based subspace separation for multiple frequency estimation," *Digit. Signal Process.*, vol. 23, no. 1, pp. 30–37, Jan. 2013.
[9] R. Yu, E. A. Ince, and A. Hocanin, "Subspace alignment and separation for multiple frequency estimation," *IEEE Signal Process. Lett.*, vol. 22, no. 1, pp. 16–20, Jan. 2015.
[10] S. Peleg and B. Friedlander, "The discrete polynomial-phase transform," *IEEE Trans. Signal Process.*, vol. 43, no. 8, pp. 1014–1901, Aug. 1995.
[11] S. Liu, Y. Ma, and T. Shan, "Segmented discrete polynomial-phase transform with coprime sampling," *J. Eng.*, vol. 2019, no. 19, pp. 5619–5621, Oct. 2019.

[12] S. Djukanović and V. Popović-Bugarin, ''Efficient and accurate detection and frequency estimation of multiple sinusoids,'' *IEEE Access*, vol. 4, pp. 1–8, 2018.
[13] V. Popović-Bugarin and S. Djukanović, ''A low complexity model order and frequency estimation of multiple 2-d complex sinusoids,'' *Digit. Signal Process.*, vol. 104, pp. 1–9, 2020, Art. no. 102794.
[14] J. M. Papy, L. De Lathauwer, and S. Van Huffel, ''Exponential data fitting using multilinear algebra: The single-channel and multi-channel case,'' *Numer. Linear Algebra with Appl.*, vol. 12, no. 8, pp. 809–826, 2005.
[15] E. A. Ince, M. K. Allahdad, and R. Yu, ''A tensor approach to model order selection of multiple sinusoids,'' *IEEE Signal Process. Lett.*, vol. 25, no. 7, pp. 1104–1108, Jul. 2018.
[16] K. N. Mokios, N. D. Sidiropoulos, M. Pesavento, and C. E. Mecklenbrauker, ''On 3D harmonic retrieval for wireless channel sounding,'' in *Proc. IEEE Int. Conf. Acoust., Speech, Signal Process.*, Montreal, QC Canada, May 2004, pp. 1189–1192.
[17] M. Pesavento, C. F. Mecklenbräuker, and J. F. Böhme, ''Multidimensional rank reduction estimator for parametric MIMO channel models,'' *EURASIP J. Adv. Signal Process.*, vol. 2004, no. 9, pp. 1354–1363, Dec. 2004.
[18] R. Boyer, ''Decoupled root-MUSIC algorithm for multidimensional harmonic retrieval,'' in *Proc. IEEE 9th Workshop Signal Process. Adv. Wireless Commun.*, Recif, Brazil, Jul. 2008, pp. 16–20.
[19] M. Haardt, F. Roemer, and G. Del Galdo, ''Higher-order SVD-based subspace estimation to improve the parameter estimation accuracy in multidimensional harmonic retrieval problems,'' *IEEE Trans. Signal Process.*, vol. 56, no. 7, pp. 3198–3213, Jul. 2008.
[20] C. Hu, Y. Wu, L. Huang, and G. Yan, ''Unitary root-MUSIC based on tensor mode-R algorithm for multidimensional sinusoidal frequency estimation without pairing parameters,'' *Multidimens. Syst. Signal Process.*, vol. 31, no. 2, pp. 491–501, Apr. 2020.
[21] J. P. C. L. Costa, F. Roemer, M. Haardt, and R. T. Sousa, ''Multi dimensional model order selection,'' *EURASIP J. Adv. Signal Process.*, vol. 2001, no. 1, pp. 1–13, 2011, Art. no. 26.
[22] D. Rife and R. Boorstyn, ''Single tone parameter estimation from discrete-time observations,'' *IEEE Trans. Inf. Theory*, vol. 20, no. 5, pp. 591–598, Sep. 1974.
[23] L. Lathauwer, B. Moor, and J. Vandewalle, ''A multilinear singular value decomposition,'' *SIAM J. Matrix Anal. Appl.*, vol. 21, no. 4, pp. 1253–1278, 2000.
[24] S. Lloyd, ''Least squares quantization in PCM,'' *IEEE Trans. Inf. Theory*, vol. 28, no. 2, pp. 129–137, Mar. 1982.
[25] I. Csiszar, ''Why least squares and maximum entropy? An axiomatic approach to inference for linear inverse problems,'' *Annu. Statist.*, vol. 19, no. 4, pp. 2032–2066, 1991.
[26] M. G. Christensen, A. Jakobsson, and S. H. Jensen, ''Sinusoidal order estimation using angles between subspaces,'' *EURASIP J. Adv. Signal Process.*, vol. 2009, no. 1, pp. 1–11, Dec. 2009.
[27] M. P. Atre and S. Apte, ''Mathematical analysis of acoustic guitar notes,'' *Int. J. Signal Process.*, vol. 2, pp. 21–27, Jan. 2017.
[28] J. F. Alm and J. S. Walker, ''Time-frequency analysis of musical instruments,'' *SIAM Rev.*, vol. 44, no. 3, pp. 457–476, Jan. 2002.

RUNYI YU (Senior Member, IEEE) received the Ph.D. degree in automatic control from the Beijing University of Aeronautics and Astronautics, Beijing, China. He is currently a Professor of electrical and electronic engineering with the Eastern Mediterranean University, Famagusta, North Cyprus. He has authored or coauthored more than 60 publications in the general areas of systems and control and signal processing. His current research interests include sampling theory, tensor analysis, and their applications in data processing.

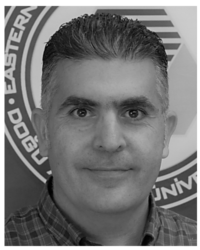

ERHAN A. INCE (Member, IEEE) was born in Nicosia, North Cyprus, in 1969. He received the B.Sc. and M.Sc. degrees in electrical engineering from Bucknell University, in 1990 and 1992, respectively, and the Ph.D. degree in communications engineering from Bradford University, in 1997. Since 1998, he has been with Eastern Mediterranean University, where he is currently a Professor with the Department of Electrical and Electronic Engineering. He has authored or coauthored more than 45 publications in the general areas of signal processing and communications. His research interests include channel coding, multi-carrier techniques, WiMAX/LTE/LTE-A/LTE-Pro, image and video processing, and statistical signal processing.